Extended Abstracts of the 2012 International Conference on Solid State Devices and Materials, Kyoto, 2012, pp298-299

High-performance high-κ $SmTiO_3$ gate dielectrics for amorphous InGaZnO thin-film transistor applications

Fa-Hsyang Chen[1], Meng-Ning Hung[1], Hung-Yu Chen[1], Jiang-Hung Liu[1], Jim-Long Her[2], Yasuhiro H. Matsuda[3], and Tung-Ming Pan[1]*

[1]Department of Electronics Engineering, Chang Gung University, Taoyuan 333, Taiwan, R. O. C.
[2] Division of Natural Science, Center for General Education, Chang Gung University, Taoyuan 333, Taiwan, R. O. C.
[3]Institute for Solid State Physics, The University of Tokyo, Chiba 277-8581, Japan
*Tel: 886-3-211-8800 Ext. 3349; Fax: 886-3-211-8507; e-mail:tmpan@mail.cgu.edu.tw

1. Introduction

The amorphous InGaZnO (α-IGZO) material has attracted much attention as active layer for next generation thin-film transistor (TFT) applications due to the transparent characteristics, high field effect mobility, and good uniformity [1]. In order to decrease the operation voltage, the high-k materials have been extensively studied as gate dielectrics for α-IGZO TFT applications [2-3]. Recently, samarium oxide (Sm_2O_3) film has been considered as a potential gate dielectric due to its high dielectric constant, wide band gap, and thermodynamically stable [4]. Additionally, it has been reported that the incorporation of Ti into lanthanide oxide exhibited better electrical characteristics [5]. In this paper, we investigated the high performance α-IGZO TFT with a high-κ $SmTiO_3$ gate dielectric for active-matrix organic light-emitting diode applications.

2. Experiment

Fig. 1 illustrates the schematic cross section of the high-κ $SmTiO_3$ α-IGZO TFT devices. The 40 nm TaN bottom gate electrodes were deposited on the thermally grown SiO_2/Si substrates by rf sputtering. The 120 nm $SmTiO_3$ films were deposited as a gate dielectric using co-sputtering. Then, samples were annealed at 400 °C by furnace in O_2 ambient for 10 min. The active layer of α-IGZO film was deposited on the dielectric film by sputtering. The thermal evaporated Al source-drain electrodes were patterned by lift-off process.

3. Result and Discussion

Fig. 2 depicts the XRD patterns that three $SmTiO_3$ (221), (311), and (132) peaks are found in the annealed film, suggesting that formation of a crystallized $SmTiO_3$ compound. The C-V curves of the Al/$SmTiO_3$/TaN capacitors are shown in Fig. 3. The dielectric constant of $SmTiO_3$ films with and without oxygen annealing is 11 and 9.2, respectively. Fig. 4 shows the Sm $3d_{5/2}$, Ti $2p_{3/2}$, and O 1*s* core level XPS spectra of the $SmTiO_3$ films. The Sm $3d_{5/2}$ peak position located at 1084.7 eV of the annealed sample is shifted to a higher binding energy by about 0.4 eV as compared to the Sm_2O_3 reference position, as shown in Fig. 4 (a). The Ti $2p_{3/2}$ peak of the annealed film is shifted to higher binding energy than the TiO_2 reference position, as shown in Fig. 4 (b). This shift was attributed to Ti in $SmTiO_3$ compound structure. The O 1*s* spectra for the $SmTiO_3$ films with/without oxygen annealing are shown in Fig. 4 (c). The O 1s signal comprised three peaks at 530.4, 531.4, and 532.8 eV, which we assign to Sm_2O_3, $SmTiO_3$, and nonlattice, respectively. The O 1s peak intensity corresponding to $SmTiO_3$ for the annealed film is larger than that of as-deposited film.

Fig. 5 and 6 demonstrate the transfer characteristics and output characteristics for the $SmTiO_3$ α-IGZO TFT devices with/without oxygen annealing, respectively. After oxygen annealing, the $SmTiO_3$ α-IGZO TFT exhibited good electrical characteristics, including low threshold voltage (V_{TH}) of 0.27 V, large field-effect mobility of 10.9 cm^2/V-s, small subthreshold swing (S.S.) of 184 mV/dec, and high I_{on}/I_{off} ratio of 3.2×10^7. Fig. 7 shows the threshold voltage variations as a function of the stress time for the $SmTiO_3$ α-IGZO TFT devices. The TFT device with oxygen annealing exhibited lower shift than that without oxygen annealing, suggesting the low number of negative charges in the $SmTiO_3$ dielectric and/or the interface of $SmTiO_3$ and IGZO layer. The corresponding schematic band diagram of a $SmTiO_3$ α-IGZO TFT device is shown in Fig 8. The measured and extracted key parameters are summarized in Table 1, where the data from α-IGZO TFT devices incorporating HfO_2 [2], Al_2O_3/SiN_x [3], SiO_2 [6] and SiN_x [7] gate dielectrics are shown for comparison.

4. Conclusion

We investigated high performance high-κ $SmTiO_3$ α-IGZO TFT device with oxygen annealing. The high-κ Sm_2O_3 α-IGZO TFT device exhibited a low threshold voltage of 0.27 V, large mobility of 10.9 cm^2/V-s, small S.S. of 184 mV/dec and high I_{on}/I_{off} current ratio of 3.2×10^7. The high-κ $SmTiO_3$ gate dielectric is a suitable material to fabricate high performance α-IGZO TFTs.

Acknowledgements

The Chang Gung University group was supported by the National Science Council (NSC), Taiwan, under contract no. NSC-98-2221-E-182-056-MY3.

References

[1] M. C. Hung, H. T. Hsiao, W. T. Lin, C. H. Tu, J. J. Chang, and P. L. Chen, Jpn. J. Appl. Phys. **50** (2011) 03CB07.
[2] L. Yuan, X. Zou, G. Fang, J. Wan, H. Zhou, and X. Zhao, IEEE Electron Device Lett. **32** (2011) 42.
[3] J. M. Lee, I. T. Cho, J. H. Lee, W. S. Cheong, C. S. Hwang, and H. I. Kwon, Appl. Phys. Lett. **94** (2009) 222112.
[4] T. M. Pan and F. H. Chen, Semicond. Sci. Technol. **26** (2011) 045004.

[5] R. B. van Dover, Appl. Phys. Lett. **74** (1999) 3041.
[6] W. Lim, E. A. Douglas, D. P. Norton, S. J. Pearton, F. Ren, Y. W. Heo, S. Y. Son, and J. H. Yuh, Appl. Phys. Lett. **96** (2010) 053510.
[7] G. H. Kim, B. D. Ahn, H. S. Shin, W. H. Jeong, H. J. Kim, and H. J. Kim, Appl. Phys. Lett. **94** (2009) 23350.

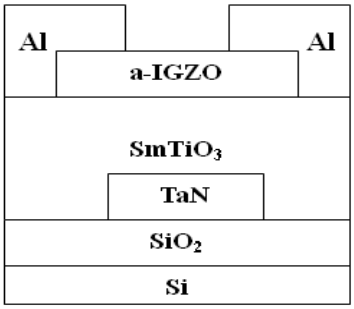

Fig. 1. Schematic diagram of the high-κ $SmTiO_3$ α-IGZO TFT devices.

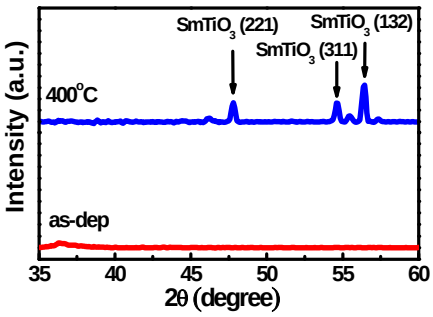

Fig. 2. XRD patterns of $SmTiO_3$ dielectric films with/without oxygen annealing.

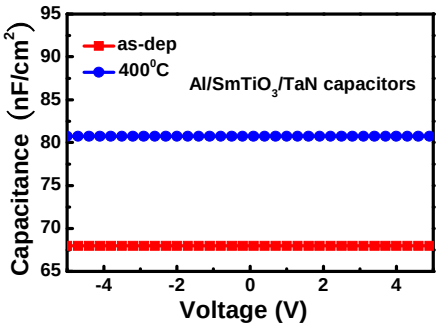

Fig. 3. C-V curves of Al/$SmTiO_3$/TaN capacitors with/without oxygen annealing.

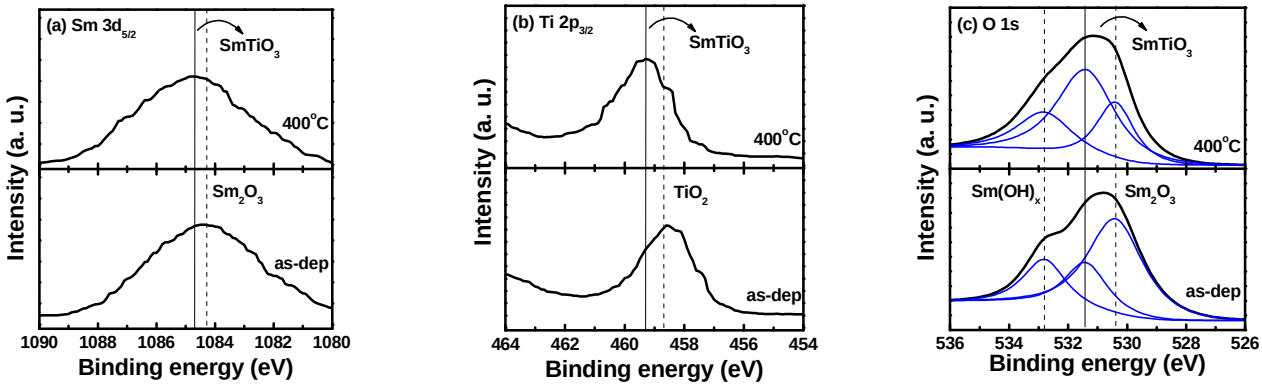

Fig. 4. XPS spectra displaying the (a) Sm $3d_{5/2}$, (b) Ti $2p_{3/2}$, and (c) O1*s* energy levels in high-k $SmTiO_3$ films with/without annealing.

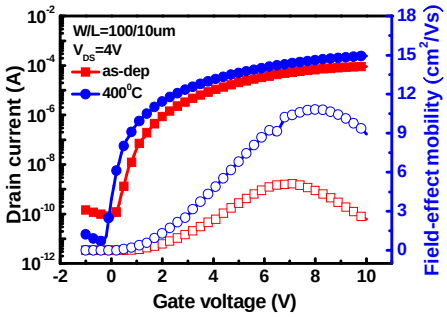

Fig. 5. Transfer characteristics and field-effect mobility versus gate voltage for high-k $SmTiO_3$ α-IGZO TFT devices with/without oxygen annealing.

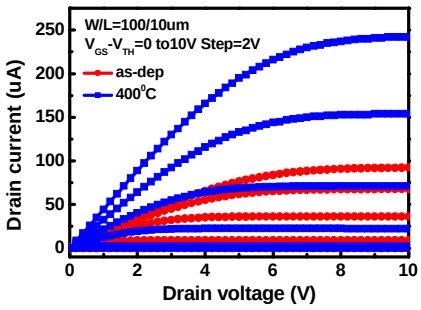

Fig. 6. Output characteristics for high-k $SmTiO_3$ a-IGZO TFT devices with/without oxygen annealing.

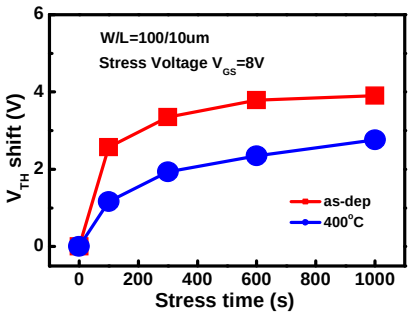

Fig. 7. Threshold voltage shift versus stress time for high-κ $SmTiO_3$ α-IGZO TFT devices with/without oxygen annealing.

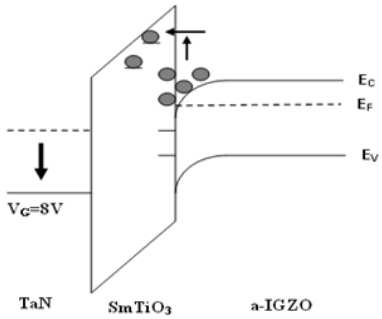

Fig. 8. The schematic band diagram of α-IGZO TFT devices with $SmTiO_3$ dielectric under V_{GS}=8V stress.

Table I. Comparison of key parameters for α-IGZO TFTs fabricated with a $SmTiO_3$, HfO_2, Al_2O_3/SiN_x, SiO_x, and SiN_x.

Gate oxide	V_{max} (V)	V_{TH} (V)	$\mu_{F.E.}$ (cm^2/V-s)	S.S. (V/dec)	I_{on}/I_{off}
$SmTiO_3$ 400 °C	10	0.27	10.9	0.18	3.2×10^7
$SmTiO_3$ as-dep	10	0.75	5.2	0.30	1.2×10^6
HfO_2 [2]	5	-1.00	8.4	0.24	1.2×10^6
Al_2O_3/SiN_x [3]	15	1.00	16.5	0.24	$>1.0\times10^9$
SiO_x [6]	15	0	2.1	0.74	1.0×10^5
SiN_x [7]	30	15.84	0.6	2.81	4.6×10^6